13th Australasian Fluid Mechanics Conference
Monash University, Melbourne, Australia
13-18 December 1998

EXPERIMENTS ON LOCAL BOUNDARY-LAYER RECEPTIVITY TO CONVECTED VORTICITY

Anthony J. DIETZ

MCAT Inc., NASA Ames Research Center
Moffett Field, California, USA

ABSTRACT

A review of the results from a series of experiments investigating the receptivity of a Blasius boundary layer to a number of different convected disturbances is presented. Harmonic, pulse and random two-dimensional disturbances were introduced by a vibrating ribbon positioned upstream of a flat plate. Two-dimensional roughness elements provided a receptivity site on the plate. A three-dimensional disturbance was generated by the pulsed displacement of a small wing. Finally the response of the boundary layer to turbulent fluctuations in the ribbon wake was measured.

INTRODUCTION

Accurate prediction of boundary-layer transition is crucial to the solution of a wide range of fluid dynamics problems, from the design of low-drag airfoils to the estimation of re-entry heat loads. In many flows transition begins with a receptivity process, in which boundary-layer instabilities are excited by disturbances in the freestream. However, as the long wavelength freestream disturbances cannot directly excite the short wavelength instability waves, the receptivity problem becomes one of wavelength conversion. Goldstein (1983) showed that a wavelength conversion mechanism exists in the rapidly growing boundary layer in the leading-edge region. Goldstein (1985) and others also showed that wavelength conversion occurs in local regions with short-scale perturbations of the boundary-layer mean flow, such as at roughness elements or suction strips. Reviews of more recent extensions to the early theories are given in Kerschen (1990), Choudhari (1994) and Crouch (1994). The theoretical analyses suggested that the following expression can be used to model the local receptivity:

$$u'_{ts} = u'_{fs} F(\alpha_{ts} - \alpha_{fs})\, \Lambda(F,R) \qquad (1)$$

where u'_{ts} is the instability amplitude, u'_{fs} is the amplitude of the streamwise fluctuations at the edge of the boundary layer, $F(\alpha_{ts}-\alpha_{fs})$ is the spatial Fourier transform of the surface geometry, evaluated at a wavenumber equal to the difference between the instability wavenumber and the freestream wavenumber, and $\Lambda(F,R)$ is an efficiency function, which varies with frequency and Reynolds number but is independent of the surface geometry.

Despite a significant body of experimental evidence for local receptivity to acoustic disturbances (e.g. Wiegel & Wlezien, 1996), the series of experiments described in this paper were the first experimental confirmation of local receptivity to convected disturbances.

EXPERIMENTAL METHOD

The experiments were conducted in a low-turbulence research wind tunnel in the Fluid Mechanics Laboratory at the NASA Ames Research Center. Detailed descriptions of the facility and experimental technique are given in Dietz (1996,1997). Measurements were made on a polished aluminium plate, 1.2 m long, 0.38 m wide, with a 58:1 elliptical leading edge. A zero pressure gradient (Blasius) boundary layer was obtained by setting the plate at a slight angle of attack to negate the effects of the growing wall boundary layers. A flap at the rear of the plate was used to fix the stagnation point on the leading edge. Vortical disturbances were introduced into the freestream by a vibrating ribbon, mounted 0.58 m upstream of the plate leading edge. A local receptivity site was provided by strips of 25.4 mm wide, 50 μm thick polyester tape applied to the plate surface in the vicinity of the first branch of the neutral stability curve (branch 1). Streamwise velocity measurements were made using a traverse mounted hotwire probe. A second probe was positioned at the edge of the ribbon wake to provide a reference for phase measurements. This wire was offset 0.5m in the spanwise direction. The experimental set-up is shown in Figure 1.

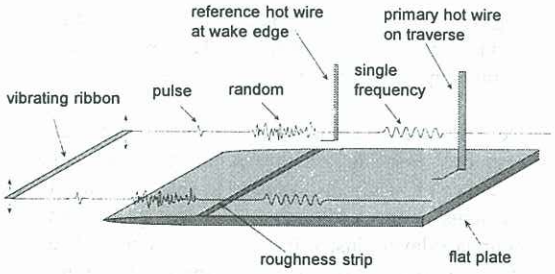

Figure 1: Schematic of experimental set-up.

As the instability waves at the roughness location were too small to be detected, the waves were measured at a downstream location where the exponential growth of the waves had increased their amplitudes to measurable levels. Amplification factors calculated using linear stability theory were then used to determine the initial wave amplitudes at the receptivity site. The experiments were conducted at a nondimensional frequency $F=2\pi fv/U_\infty^2 \times 10^6 = 50$, and a branch 1 Reynolds number

$R=\sqrt{(Re)} = \sqrt{(U_x x/\nu)} = 613$, giving a freestream velocity $U_x = 17$ m/s and a frequency $f = 157$ Hz, at a temperature of 288K and a dynamic viscosity $\nu = 1.455\times10^{-5}$ m^{2}s^{-1}. The experiment was controlled to maintain a constant R and F by adjusting the freestream velocity and the ribbon forcing frequency as the flow temperature and the atmospheric pressure varied. At these conditions, the turbulence intensity in the freestream and in the boundary layer remained below 0.1%. The ribbon amplitude was set to give a streamwise fluctuation amplitude of 0.3% at the edge of the boundary layer.

RESULTS

The convected disturbance produced by the vibrating ribbon is shown in Figure 2, where streamwise velocity spectra recorded at a number of points in and above the boundary layer are plotted. The profile of the harmonic disturbance peaks in the high shear region on either side of the wake and then decays exponentially. It persists beyond the turbulent wake and proves to be an effective way to excite the boundary layer with a single wavenumber convected disturbance. Inside the boundary layer the disturbance is rapidly damped towards the wall. Although some energy is present in the second and third harmonics of the forcing frequency, tensioning the ribbon has reduced these to acceptable levels.

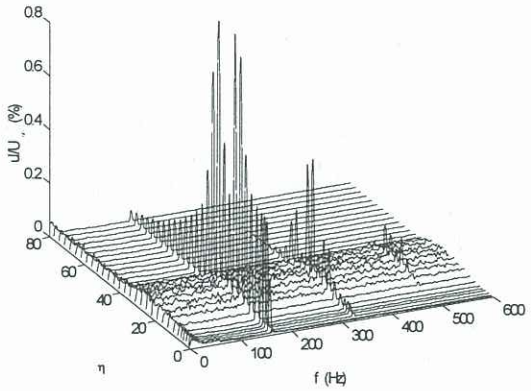

Figure 2: Streamwise velocity spectra recorded at R=633 and plotted against the boundary layer reference co-ordinate $\eta = y/\sqrt{(2\nu x/U)}$.

Downstream measurements of the boundary-layer response with no roughness on the plate found no evidence of instability waves. However, when roughness elements were added in the vicinity of branch 1, boundary-layer instabilities were excited. The mode shape, growth rate and phase speed of the instability waves matched that of the Tollmien Schlicting (TS) waves predicted by linear stability theory. Linear stability calculations were then used to determine the immeasurably small initial amplitudes of the waves at the roughness location from the amplitudes measured downstream; separating the receptivity (generation) characteristics of the waves from their stability (growth) characteristics. The variation of the TS amplitude with roughness location is shown in figure 3a. Estimates of the amplitude at the roughness location and also of the effective amplitude at branch 1 are given for each roughness location. The amplitude at the roughness location increases as the roughness is moved towards the leading edge. However, upstream of branch 1 the waves decay and so the effective branch 1 amplitude is maximum for roughness elements located slightly upstream of branch 1.

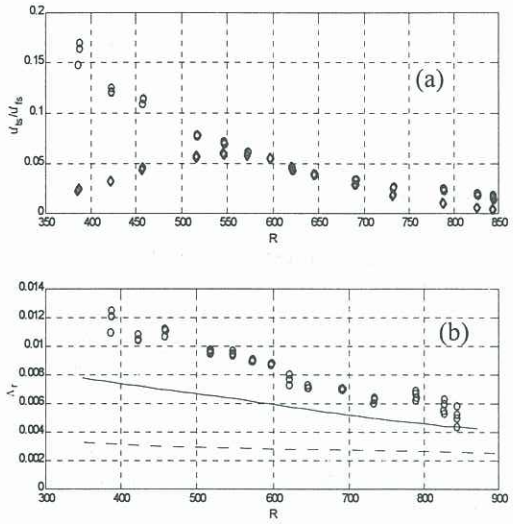

Figure 3: (a) TS amplitude variation with Reynolds number based on roughness location: amplitude at the roughness location (o); effective amplitude at the branch I location (◊). (b) Receptivity efficiency function: measurements (o), calculations (Choudhari 1996 ,—), asymptotic theory (Kerschen 1990, - - -).

Measurements showed that the receptivity varied linearly for disturbance amplitudes up to 1% of the freestream velocity, and for roughness heights up to 10% of the displacement thickness. The variation with roughness geometry was shown to be well modelled by the spatial Fourier transform, so within this linear range, equation 1 could be used to determine the receptivity efficiency function. This function is compared with vortical receptivity theory and calculations in Figure 3b. The experiments are in reasonable agreement with the calculations considering the extreme sensitivity of the stability characteristics of a Blasius boundary layer and the limitations of the theory. A complete account of this experiment is given in Dietz (1998a).

However, these results apply to continuous single-frequency waves while real world flows contain broadband transient disturbances. Experiments with broadband pulse and random disturbances were reported by Dietz (1998b). The response to a pulse disturbance is shown in Figure 4 where a TS wave packet, generated by the interaction between a convected pulse and distributed surface roughness, can be seen lagging the pulse disturbance. The lower propagation speed of the wave packet has separated the two phenomena allowing each to be analyzed independently.

In Figure 5 the amplitude of the pulse through the boundary layer is compared to the profile measured with single-frequency excitation. The measured profiles agree well with the results of an unsteady boundary layer

calculation with streamwise forcing as the upper boundary condition. In Figure 6 the profile of the maximum amplitude in the packet is compared with the mode shape of the TS waves excited by single-frequency disturbances and also with the TS eigenvector from linear stability theory. Again, there is good agreement between the profiles.

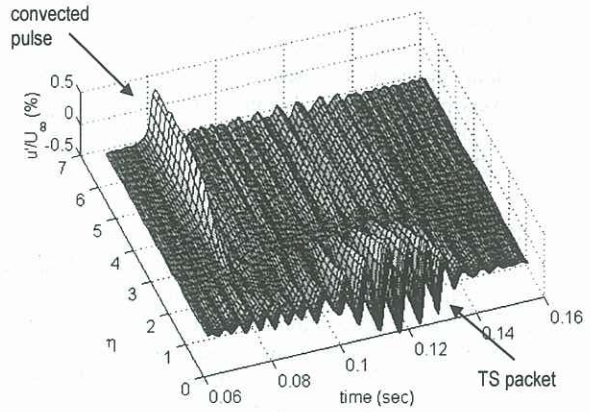

Figure 4: Boundary-layer response to a pulse disturbance. Phase-locked averaged time records of the streamwise velocity fluctuations measured at a number of heights through the layer. Array of 10 roughness elements. R=900.

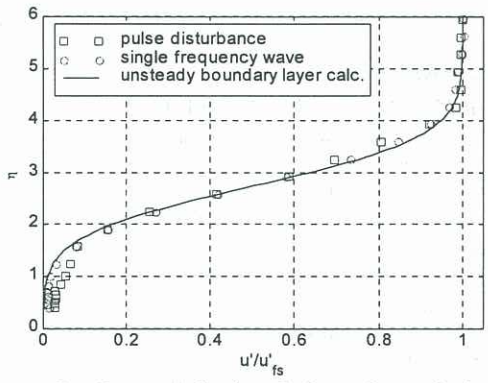

Figure 5: Rms amplitude of the pulse and single-frequency disturbances in the boundary layer compared with calculations by Choudhari (1996). R=640.

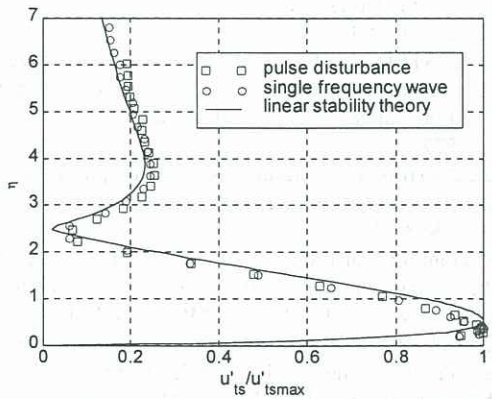

Figure 6: TS eigenvector excited by pulse and single-frequency disturbances at distributed roughness compared with e^N calculations (Malik 1989), R=900.

The receptivity coefficients for pulse and random disturbances were determined by using linear stability calculations to refer the spectra measured downstream back to the roughness location at branch 1. The spectra were then divided by the spectra of the freestream disturbance . The coefficients so obtained are compared with single-frequency results in Figure 7. The results are in agreement for all three disturbance types. The two plots confirm theoretical predictions that receptivity to distributed roughness is nearly an order of magnitude greater than that for single roughness, and that results for distributed roughness are highly tuned to a resonant frequency where waves generated at successive roughness elements are in phase and add constructively. These comparisons demonstrate that the receptivity theory is equally applicable to single-frequency and broadband disturbances.

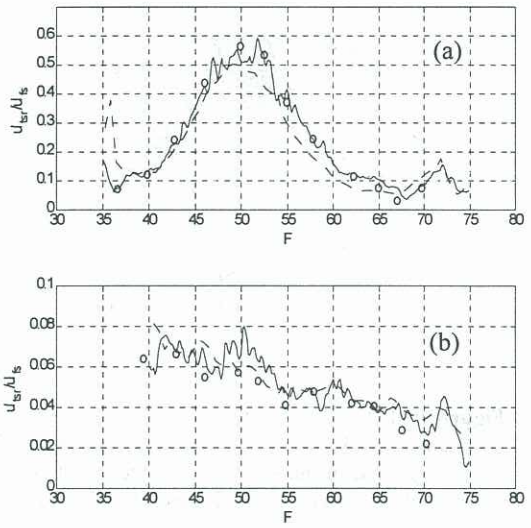

Figure 7: Boundary-layer receptivity for single frequency (o), pulse (-) and random (---) disturbances. (a) distributed roughness, (b) single roughness.

In the next series of tests the ribbon was replaced by a narrow wing to introduce a three-dimensional convected disturbance. The response of the boundary layer to this disturbance is shown in Figure 8.

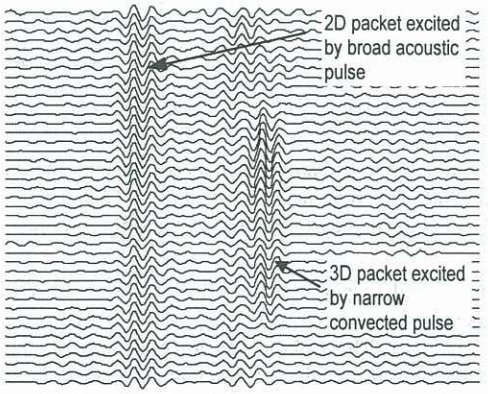

Figure 8: Boundary-layer response to an acoustic pulse and convected 3D pulse. Phase-locked averaged time traces measured on a spanwise line at constant height in the boundary layer. Filtered 100-200Hz. Single roughness.

The pulse displacement of the wing generated a broad acoustic pulse and a narrow convected pulse. The acoustic pulse reached the roughness first and excited a two-dimensional wave packet. The convected disturbance then excited a three-dimensional packet when it passed over the roughness at a later time. The advantage of using pulsed disturbances, suggested by Saric (1995), was realised in this experiment as the two packets were indistinguishable when excited by continuous forcing. The streamwise growth of the packets is shown in Figure 9. The growth of the two packets was similar and matched that predicted by linear stability theory for a wave of the dominant frequency in the packet. This suggests the three-dimensional packet was dominated by two-dimensional modes as a packet excited by a point source would grow at a slower rate than a two-dimensional packet due to the influence of oblique modes.

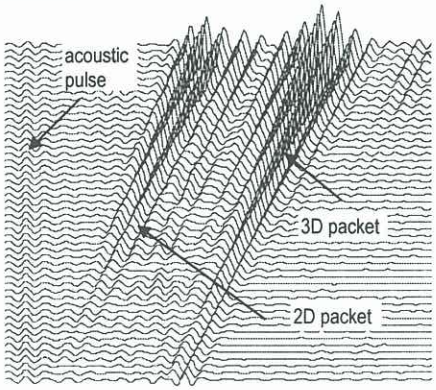

Figure 9: Boundary-layer response to an acoustic pulse and convected 3D pulse. Phase-locked averaged time traces measured in the streamwise direction at constant height in the boundary layer. Filtered 100-200Hz.

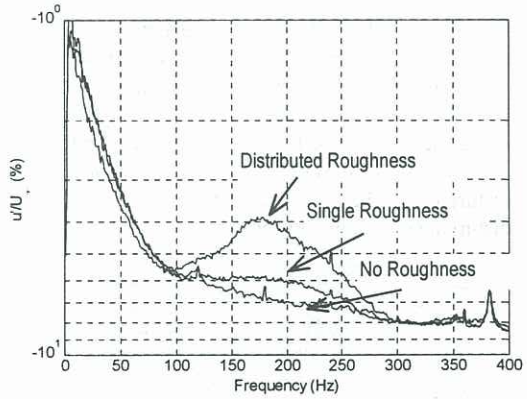

Figure 10. Streamwise velocity spectra measured at R=900, η = 0.5, with ribbon lowered so the boundary layer is excited by turbulence in the ribbon wake.

The final experiment in this series was aimed at measuring the local receptivity of the boundary layer to turbulence. The ribbon was lowered until its turbulent wake grazed the edge of the boundary layer. Turbulence in the ribbon wake was used instead of grid turbulence because the wake did not directly impact the leading edge and this reduced contributions from the leading-edge receptivity mechanism. As shown in Figure 10, the boundary layer did become receptive to the turbulent fluctuations in the wake when roughness was added to the plate. Higher amplitudes and increased tuning are apparent in the distributed roughness result compared to the single roughness result. Interactions between turbulent fluctuations in the wake and the two-dimensional roughness resulted in random three-dimensional wave packets. The growth rate of the packets was significantly lower than that measured for two-dimensional waves indicating the presence of oblique modes in the packets. The random nature of the packets prevented calculation of the packet growth rate via modal decomposition. This would be required to determine a receptivity coefficient.

CONCLUSION

Measurements of the receptivity of a laminar boundary layer to various convected disturbances at two-dimensional surface roughness confirmed many aspects of vortical receptivity theory. The theory was shown to apply equally to single-frequency and broadband disturbances. The receptivity of the boundary layer to three-dimensional disturbances and to turbulent fluctuations was also demonstrated. This experimental verification is a step towards the still unrealised goal of transition criteria that include freestream disturbance characteristics.

This work was performed while the author held a National Research Council Research Associateship.

REFERENCES

CHOUDHARI, M., & STREETT, C. L., "Theoretical prediction of boundary layer receptivity," AIAA 94-2223, June 1994.

CHOUDHARI, M., "Boundary-layer receptivity to three-dimensional unsteady vortical disturbances in free stream,' AIAA Paper 96-0181, January 1996.

CROUCH, J. D., "Theoretical studies on the receptivity of boundary layers," AIAA 94-2224, June 1994.

DIETZ, A. J., "Local boundary-layer receptivity to a convected freestream disturbance," accepted for publication in *J. Fluid Mech.*, 1998.

DIETZ, A. J., "Boundary-layer receptivity to transient convected disturbances," AIAA J., **36**, 1171-1177, 1998.

GOLDSTEIN, M. E., "The evolution of Tollmien-Schlichting waves near a leading edge," *J. Fluid Mech.*, **127**, 59-81, 1983.

GOLDSTEIN, M. E., "Scattering of acoustic waves into Tollmien-Schlichting waves by small streamwise variations in surface geometry," *J. Fluid Mech.*, **154**, 509-529, 1985.

KERSCHEN, E. J., "Boundary layer receptivity theory," *Appl. Mech. Rev.*, **43**, S152-S157, 1990.

MALIK, M. R., "e^{Malik} a new spatial stability analysis program for transition prediction using the e^N method," High Tech. Corp., HTC-8902, Hampton, VA, 1989.

SARIC, W. S., WEI, W., RASMUSSEN, B. K., & KRUTKOFF, T. K., "Experiments on leading-edge receptivity to sound," AIAA 95-2253, June, 1995.

WIEGEL, M., & WLEZIEN, R., "Acoustic receptivity of laminar boundary layers over wavy walls," AIAA Paper 93-3280, July 1993.